Developments in the Built Environment 20 (2024) 100545

Contents lists available at ScienceDirect

Developments in the Built Environment

journal homepage: www.sciencedirect.com/journal/developments-in-the-built-environment

Effect of accelerated carbonation on fine cement paste aggregates

Marión Bustamante [a], Viviana Letelier [b,e,*], Bruno Wenzel [b], Cristian Torres [b], Estefania Loyola [c], José Marcos Ortega [d]

[a] Doctoral Program in Engineering at the MacroFacultad de Ingeniería UFRO-UBB-UTAL, Temuco, 4780000, Chile
[b] Department of Civil Engineering, Universidad de La Frontera, Temuco, 4780000, Chile
[c] Department of Construction Engineering and Management, School of Engineering, Pontificia Universidad Católica de Chile, Santiago, 8320000, Chile
[d] Departamento de Ingeniería Civil, Universidad de Alicante, Alacant, 03080, Spain
[e] Concrete Innovation Hub UC (CIHUC), Pontificia Universidad Católica de Chile, Santiago, 7820436, Chile

ARTICLE INFO

Keywords:
Accelerated carbonation
Recycled aggregate
Mortar
Cement paste aggregates

ABSTRACT

Accelerated carbonation is suggested as a potential alternative for carbon dioxide sequestration, which also improves the microstructure of recycled concrete aggregates. In this study, the carbonation parameters of model aggregates derived from cement pastes with two different water/cement ratios (i.e., 0.5 and 0.7) were evaluated in order to maximize the benefits of the carbonation process on their density and absorption. For this purpose, in a first phase, the initial moisture content of the model aggregates and the reaction time were evaluated. Furthermore, in a second phase of mortar production, the fraction of fine natural aggregates was replaced, considering each type of unprocessed and carbonated model aggregate at volumetric replacement percentages of 50% and 100%, varying the amount of water in the mortar mix to maintain a similar workability in all the series. In this way, the properties of the eight series of mortars are evaluated in comparison with the control series made only with natural aggregates. The results indicate that the accelerated carbonation process positively influences density and absorption in the model aggregate. Regarding the parameters of the accelerated carbonation environment analyzed, for a higher w/c ratio in the original model aggregate, higher initial water content was necessary for the carbonation process to be efficient. As for the mechanical performance of the mortars with model aggregate, the series that incorporated model aggregate aggregates with a w/c ratio of 0.5 achieved better mechanical behavior compared to the series replacing model aggregate with a w/c ratio of 0.7; this was related to the formation of a more compact matrix in the mortar with model aggregate of cementitious pastes.

1. Introduction

In recent decades, the use of recycled aggregates has become increasingly important due to the need to address the problem of construction and demolition waste (CDW) from industry and as a strategy to meet the sector's imperative demand for raw materials from natural resources (Illankoon and Tam, 2021). The annual demand for natural aggregates (NA) in the global construction market is estimated to be more than 40 billion tons (Hawileh et al., 2023). This demand has led to the study of recycled aggregates from different sources (Kurda, 2021), including recycled concrete aggregates (RCA), one of the main components of CDW (Zhang et al., 2019), (Akhtar and Sarmah, 2018). The old adhered mortar (OAM) on the surface of RCAs can facilitate a reaction with ambient carbon dioxide. This reaction capacity is higher in fine recycled concrete aggregate (FRCA), mainly because the fine fraction has a higher specific surface area and contains a higher proportion of old adhered mortar, which can increase the contact with CO_2. Therefore, the carbonation process is a method for improving (Li et al., 2022) and transforming this characteristic of recycled aggregates into a potential alternative in the quest for carbon neutrality (Xiao et al., 2022). According to Zadeh et al. (2021), carbonation is the most effective and feasible method for improving the mechanical properties and durability of RCA by enhancing both the new interfacial transition zone (ITZ) and those already present in the RCA (Zadeh et al., 2021). Through carbonation, it is expected that CO_2 reacts with the calcium hydroxide ($Ca(OH)_2$) and calcium silicate hydrate (CSH) present in the old adhered mortar on the RCA, forming calcium carbonate ($CaCO_3$) and silica gel (SiO_2), according to the following equations (Luković, 2016):

$$Ca(OH)_2 + CO_2 \rightarrow CaC0_3 + H_2O \quad \text{Equation 1}$$

* Corresponding author. Department of Civil Engineering, Universidad de La Frontera, Temuco, 4780000, Chile.
E-mail address: vivana.letelier@ufrontera.cl (V. Letelier).

https://doi.org/10.1016/j.dibe.2024.100545
Received 17 June 2024; Received in revised form 6 September 2024; Accepted 12 September 2024
Available online 13 September 2024

$$(CaO)_x\ (SiO_2\ )(H_2O) + xCO_2 \rightarrow xCaC0_3 + SiO_2(H_2O)t + (z-t)nH_2O$$

Equation 2

Several studies have shown that carbonation improves the properties of various aggregates, including high-porosity aggregates as they can provide a considerable amount of space for CO_2 storage, making them a viable alternative to natural aggregates in concrete. Mi et al. (2023) studied a new CO_2 sequestering method by utilizing different porous aggregates such as coral aggregates, waste clay brick aggregates, lightweight aggregates. This process is divided into two stages, the first consisting of pre-soaking the aggregates in an alkaline slurry and the second consisting of curing the pre-soaked aggregates in a carbonation tank. The results indicate that the proposed CO2 sequestration method does not affect the strength development of the concrete or the pH of the concrete pore solution (Mi et al., 2023a). In terms of property improvement, using the same method in which coral aggregates were pre-soaked in $Ca(OH)_2$ slurries with different solid-to-liquid ratios (i.e. 0.2, 0.4 and 0.6 g/mL) followed by accelerated carbonation. The compressive strength of aggregates in concrete increased by up to 16% when the solid-to-liquid ratio was 0.2 g/mL compared to that before CO2 sequestration, with the opposite effect when the ratio was 0.6 g/mL (Mi et al., 2023b). In the case of accelerated wet carbonation, Xiao et al. (2022) studied this method in coarse RCA (CRCA) and FRCA aggregates, analyzing how carbonation affects their properties (Xiao et al., 2022). In this case, carbonation was carried out at a relative humidity of 75 ± 5% to accelerate the reaction process and a CO_2 concentration of 20 ± 2% already preset before the fine aggregate was introduced. Different from the case of Fang et al. (2021), who injected the gas at a rate of 0.2 L/min of CO_2 for 10 min (Fang et al., 2021). However, in both cases, a reduction in the amount and volume of pores in the recycled aggregates was reported, due to a densification of the surface of the recycled aggregates. This property improved the performance of the new pastes in both studies. In the case of Fang et al. (2021), they indicated that the application of wet carbonation resulted in a 30.8% increase in compressive strength and significant improvements in the drying shrinkage performance of the new mortar samples (Fang et al., 2021). Similarly, Xiao et al. (2022) reported that the mechanical properties and shrinkage behavior of carbonated fully recycled fine aggregate concrete are similar to those of natural aggregate concrete, replicating these results for shrinkage deformation (Xiao et al., 2022). Although true, it has been possible to corroborate the improvement of the properties of FRCA from the treatment with carbon dioxide. Due to their heterogeneity, the parameters required to achieve a correct reaction between the cement paste present in the recycled aggregates and carbon dioxide differ from each other (Poon et al., 2023). There are studies in the literature in which it can be seen that even when two aggregates of a similar size are compared, the sequestration capacity of the aggregates can be different; this is because the composition of the old mortar adhered to recycled aggregates can be very diverse due to different factors (aging, environmental circumstances during disposal, composition of the original cement used, etc.). The water-cement ratio is a critical factor in concrete strength. Depending on this ratio, two extreme situations arise. Firstly, when extremely low water-cement ratios are used, the mortar loses workability, failing to adequately fill or cover the aggregate surfaces. Consequently, the matrix strength is compromised due to weak interfacial transition zones (ITZ). Secondly, higher water-cement ratios enhance mortar workability, but the resulting layer becomes very thin and may detach from the aggregate (Xiao, 2018). In this regard, J. Xiao et al. (2013) which carried out a parametric study to analyze the effects of ITZ and new mortar matrix on the stress-strain ratio of Modeled Recycled Aggregate Concrete observed that the maximum stress and strain increased with decreasing water-cement ratio of the new mortar matrix (Xiao et al., 2013).

Thus, the present study aims to evaluate the effect of cement paste bonded to recycled concrete aggregates in the proposed accelerated carbonation process as an alternative for CO2 sequestration in the literature by comparing the water-cement ratio. This characteristic is a factor that impacts on the level of carbonation that can be obtained and the variation of the major mineralogical phases obtained through this process (Shen et al., 2022), (Georget et al., 2020). The present study aims to evaluate the effect of cement paste adhered to recycled concrete aggregates on the accelerated carbonation process proposed, as an alternative for CO_2 sequestration in the literature.

For this, two model aggregates, made of two different types of cement pastes with different water-cement ratios, were produced and subjected to an accelerated carbonation process in order to promote the use of the fine fraction of the recycled aggregates and simultaneously exploit the CO_2 reactivity. Finally, research was carried out on the performance of these unprocessed and carbonated cement paste aggregates in mortars with 50% and 100% volume replacements of natural aggregates.

2. Materials and methods

2.2. Methods

The present study was conducted in two methodological phases. In the first phase, for model aggregate from cement pastes with two water/cement ratios (i.e., 0.5 and 0.7), the optimum initial moisture content of the recycled cementitious paste aggregates was evaluated to maximize the benefits of carbonation, in terms of density and absorption of the model aggregates. Based on the selected humidity, the time in which the process was most efficient was analyzed. Then, based on the results obtained in the first phase, the moisture and time to be applied in the carbonation process were selected for each model aggregate from cement pastes with different w/c ratios used in the second phase. In the second phase, associated with the manufacture of mortars, the fraction of fine natural aggregates was replaced, considering each type of carbonated model aggregate (i.e., P05-C and P07-C) and a twin sample of these without carbonation (i.e., P05 and P07). As detailed in Table 3, the replacement percentages of fine natural aggregate (FNA) were 50% and 100% by volume.

The procedures carried out in each of the phases are detailed below.

2.1. Materials

2.1.1. Cement

Portland-pozzolan cement type IP was used according to ASTM C595 (A. (American S. for Testing y Materials)), with an initial setting time of 90 min and a final setting time of 150 min. In addition, it has a Blaine-specific surface area of 5,200 cm^2/g and a true density of 2.95 g/cm^3; its chemical composition is presented in Table 1.

2.1.2. Aggregates

In the case of the aggregate, silica sand was used. According to its particle size distribution (presented in Fig. 1), it ranged from 0.075 mm to 2.360 mm in size and its physical properties are detailed in Table 2.

Regarding the model aggregate, unlike other studies where fine recycled aggregates composed of natural aggregates were analyzed with

Table 1
Cement composition.

Composition	Cement (%)
SiO_2	38.06
Al_2O_3	8.88
CaO	40.92
Fe_2O_3	2.83
SO_3	2.33
MgO	1.59
Na_2O	1.75
K_2O	1.62
Others	1.35

Table 2
Aggregate properties.

Properties	Natural Aggregate	Cement Paste Aggregate W/C 0.5	Cement Paste Aggregate W/C 0.7	Carbonated Cement Paste Aggregate W/C 0.5	Carbonated Cement Paste Aggregate W/C 0.7
Density (g/cm^3)	2.48	1.35	1.30	1.56	1.46
Water Absorption (%)	2.17	35.60	36.50	25.50	30.30

Table 3
Detail of the proportions in the series.

Serie	Natural Aggregate	Cement Paste Aggregate W/C 0.5	Cement Paste Aggregate W/C 0.7	Carbonation process	Water/ Cement ratio
C0	100%	–	–	–	0.60
S1	50%	50%	–	Yes	0.71
S2	–	100%	–	Yes	0.90
S3	50%	–	50%	Yes	0.73
S4	–	–	100%	Yes	0.93
S5	50%	50%	–	No	0.78
S6	–	100%	–	No	0.95
S7	50%	–	50%	No	0.80
S8	–	–	100%	No	1.06

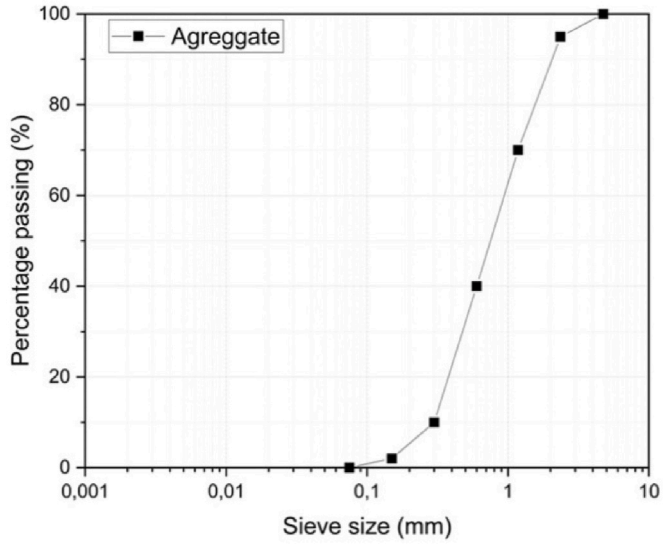

Fig. 1. Grain size distribution of natural and model aggregate used in the production process.

different percentages of OAM, in this case, model aggregate composed entirely of cement paste were analyzed. This allowed us to understand the effect of carbonation on hydrated cement products more precisely. As illustrated in Fig. 3, two aggregates of two different cement pastes were prepared, each one with different water/cement ratios (w/c). The cement pastes (60 l) were dosed in cylindrical specimens of 10 × 15 cm (Fig. 2), prepared with Type IP cement according to ASTM C595 (A. (American S. for Testing y Materials)). The first series was 0.5 w/c (P05) and the second was 0.7 w/c (P07). These cylindrical specimens were cured for 28 days at 23 °C and 90% relative humidity. Subsequently, each of the series were crushed separately through a millstone crusher, thereby obtaining the size needed for use as fine aggregates. From the series of cement pastes with a w/c ratio of 0.5, we named the fine aggregate 'P05' and, similarly, from the crushed cement pastes with a w/c ratio of 0.7, we obtained the fine aggregate 'P07'; their physical properties are detailed in Table.

2.2.1. *Phase 1 - Carbonation and aggregate preparation*

The model aggregates were subjected to an accelerated carbonation process. Due to the variability that one aggregate can have from another, it was necessary to compare and analyze different parameters in each type of model aggregate. According to Liu and Meng (2021), the characteristics of the material to be exposed to carbon dioxide play an important role in carbonation efficiency (Meng, 2021). Two parameters were considered for this study: the time exposed to the gas and the initial water content of the cement paste aggregates. The initial moisture content of the sample is one of the properties that affects the diffusion of CO_2 on the sample. If the capillary pores of the material are filled with water, the channel for CO_2 diffusion is blocked. Conversely, when these pores are drier, although CO_2 can easily diffuse into the pores, the degree of carbonation will be limited, and maximum carbonation will not be achieved. In addition, during carbonation in the presence of water, CO_2 reacts rapidly with the hydration products. Thus, when most of the surface has already reacted, this same layer may act as a barrier, hindering further diffusion of the reaction (Shtepenko et al., 2006).

Prior to the accelerated carbonation process, different percentages of water (2.5%, 5.0%, 7.5%, 10%, 20%, and 30%) were added to the model aggregates, which were in a dry state. The amount of water was applied as a percentage of the mass of the model aggregates of cement pastes with a w/c ratio of 0.5 (P05) and 0.7 (P07) that would react with CO_2

Fig. 2. Manufacture of cement paste aggregates.

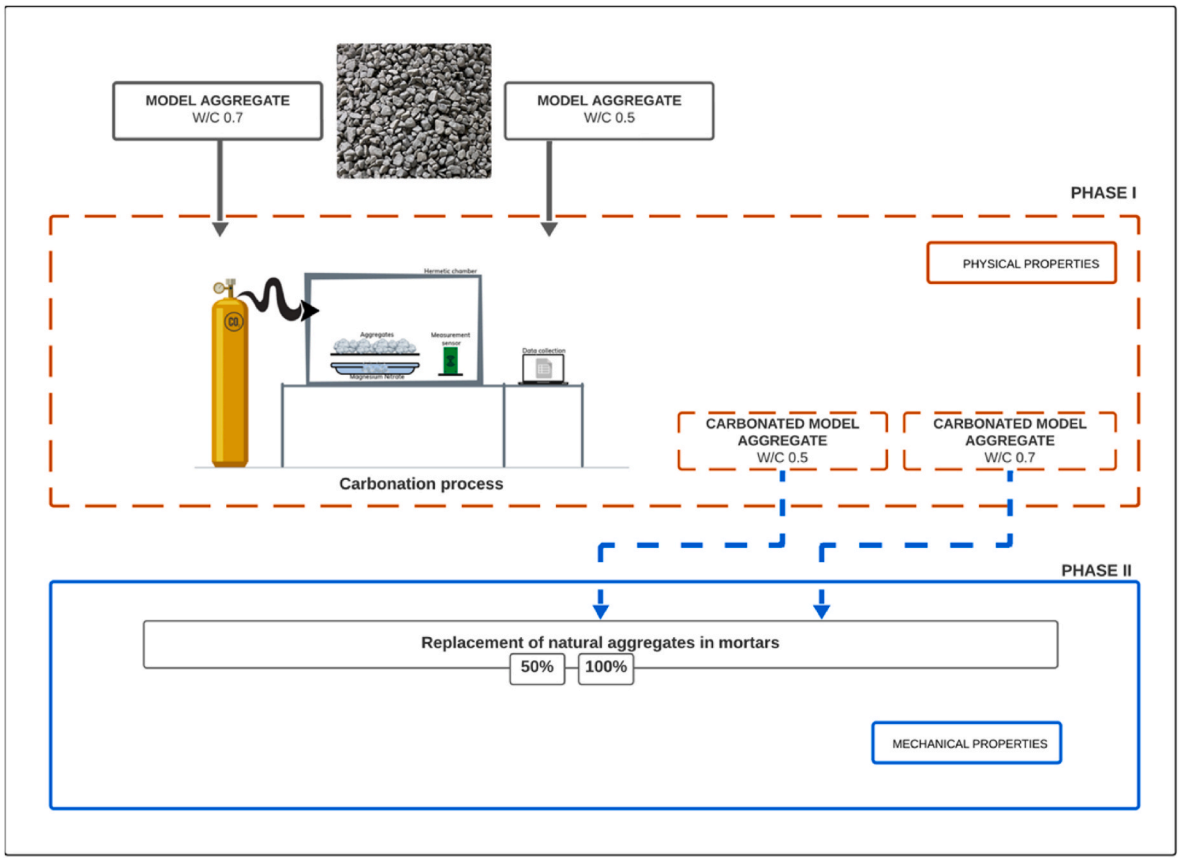

Fig. 3. Diagram of the carbonation methodology of model aggregates and their use in mortars.

inside the chamber. An accelerated carbonation time of 3 h was specified, to assess the ideal initial moisture content. For this, the model aggregates were placed in an airtight chamber (see Fig. 3) with controlled relative humidity, which can be achieved by different methods (Tam et al., 2021) using silica gel minerals, organic polymers, or inorganic solutions as in this case. Similarly to other authors (Xuan et al., 2019), (Fang et al., 2020a), a saturated saline solution of magnesium nitrate ($Mg(NO_3)_2$) according to ASTM E104 - 20a ((A. American S. for Testing y Materials)) was used to regulate the relative humidity of the environment inside the chamber to 54.4 ± 0.3% at 20 ± 2 °C.

Finally, using a carbon dioxide cylinder, the gas was injected steadily at 5 L/min until the pressure inside the chamber was 80 mbar. The pressure and humidity parameters remained constant during the time evaluated. After each test, the density properties were evaluated according to UNE-EN 1015-10 (A. E. de N. y Certificación, 2000a) and aggregate absorption was evaluated according to UNE-EN 1015-18 (A. E. de N. y Certificación, 2003). The optimal initial moisture content was chosen for model aggregates P05 and P07, based on the density and absorption data obtained. The criterion for the selection of the initial moisture content is that it was able to reduce the absorption to the highest percentage. Then, the optimal time for achieving the most efficient carbonation was evaluated, repeating the same steps from the previous stage but keeping the initial humidity constant. The times evaluated were 3, 6, and 9 h. After each test, the density and absorption properties of the aggregates were re-evaluated, selecting the time that yielded the best results. After selecting the model aggregates to be used in manufacturing mortars, X-ray diffraction analysis was performed to analyze the presence of precipitated calcium carbonates.

2.2.2. *Phase 2 - Mix proportions*

Nine mortar series were prepared to compare and evaluate the effects of carbonate model aggregates replacing natural aggregate. As shown in Table 4, for the production of mortars, FNA was replaced by normal model aggregates at 50% and 100% (by volume) in dry state. Mortars were also produced with replacement of FNA by carbonated model aggregates in the dry state, subjected to an accelerated carbonation treatment for 6 h for both cases (P05 and P07), although precipitation of carbonation products was observed after 3 h. Properties such as adsorption showed a tendency to settle after 6 h. The only difference between the two processes was in the initial water content, which was 10% for the model aggregates with a water-cement ratio of 0.5 and an initial moisture content of 20% for the model aggregates with a water-cement ratio of 0.7.

Prior to the production of the mortars, the "flow table" test described in the following section was carried out to determine the ideal water-cement ratio that would maintain the same workability.

Table 4
Mix proportions (g).

Series	Cement	Aggregates					Water
		Natural	P0.5	P0.5-C	P0.7	P0.7-C	
C00	448	1344	–	–	–	–	268.80
S1	448	672	–	419	–	–	318.08
S2	448	–	–	839	–	–	403.20
S3	448	672	–	–	–	376	327.04
S4	448		–	–	–	752	416.64
S5	448	672	419	–	–	–	349.44
S6	448	–	839	–	–	–	425.60
S7	448	672	–	–	376	–	358.40
S8	448		–	–	752	–	474.88

2.3. Testing methods

2.3.1. CO_2 sequestration capacity

To measure CO_2 sequestration capacity, a thermogravimetric analysis (TGA) was performed. According to Zhang et al. (2017), the TGA analysis can measure the CO_2 uptake of the material from the decomposition of the carbonates because it leads to a weight loss and, therefore, allows the estimation of sequestered CO_2 (Zhang et al., 2017). Thus, on this occasion, the decomposition content associated with calcite ($CaCO_3$) was calculated from thermogravimetry performed on the mortars made with the carbonated pastes (i.e., P05-C and P07-C). For this, Equation (1) was used (Wang et al., 2019), where C (%) is the mass loss attributable to decarbonization between 300 and 850 °C based on the report by Chang et al. (2016), which associates the temperature range of 500–850 °C with $CaCO_3$ and CH decomposition (Chang et al., 2016). This range has been extended because when working with model aggregates of cementitious pastes, it is possible that the reaction between CO_2 and C_2S or C_3S present in the aggregates has taken place (Rostami et al., 2012), (Fang et al., 2020b). According to Sousa et al. (2024), this reaction results in low crystallinity CSH gels with temperature ranges around 400 °C (Sousa et al., 2024). All of these products of interest because they are products of carbonation and indicate the possibilities of sequestration.

$$C_s\left(\frac{g}{kg}\right) = \frac{C(\%)}{100 - C(\%)} \times 1000 \qquad \text{Equation 3}$$

2.3.2. Density, absorption, and porosity

The real dry density was determined by the UNE-EN 1015-10 (A. E. de N. y Certificación, 2000a)standard, while water absorption and porosity were determined using UNE-EN 1015-18 (A. E. de N. y Certificación, 2003); these were tested in 3 specimens of 100 mm diameter and 50 mm height at 28 days.

2.3.3. Consistency

To adequately compare all the mortars of the different series and obtain adequate workability, the consistency was kept to a range of 205 ± 5 mm, according to NCh2256/1 ((Instituto Nacional de Normalización) INN, 2001). For this, measurements were taken using a mini slump cone with an internal diameter of 100 mm on a 250 mm flow table disc, according to UNE-EN 1015-3 (A. E. de N. y Certificación, 2000b). To carry out the procedure, the mold was first filled with the mortar in its fresh state and then lifted from the flow table, allowing the mixture to spread onto the disc. The table was then shaken 15 times at a constant rate and two perpendicular mortar diameter measurements were taken. Finally, the consistency value was determined as the measurement average of 3 samples, considering an accuracy of 1 mm.

2.3.4. Capillarity

This test aimed to determine the capillary water absorption coefficient of the mortar according to ASTM C1585 (International, 2013). For this, the increase in mass of a specimen (50 mm in height and 100 mm in diameter) was measured, exposing one of its surfaces to water while the others were waterproofed. For each series, three specimens were tested after curing for 28 days.

2.3.5. Compressive and flexural strength

The mechanical behavior of the series was determined through compressive and flexural strength tests at 7, 14, and 28 days, on 40 mm × 40 mm x 160 mm specimens, according to ASTM C39/C39M (A. (American S. for Testing y Materials), 2023) and ASTM C78/C78M (A. (American S. for Testing y Materials), 2021), respectively.

2.3.6. Ultrasonic Pulse Velocity (UPV)

The ultrasonic pulse velocity (UPV) method was used to evaluate the microstructure of the mortar. The test determines the propagation speed of longitudinal wave impulses in the mortar to evaluate the uniformity and quality of the samples, indicating the presence of voids and cracks. This test was performed on three specimens (50 mm in height and 100 mm in diameter) at 28 days of curing, according to ASTM C597-16 ((A. American S. for Testing y Materials)).

2.3.7. Thermal gravimetric analysis (TGA)

This method is an empirical technique that measures the variation of the mass of the sample when heated at a controlled rate in an appropriate environment. On this occasion, the test was performed using a TA Instruments Q600 simultaneous thermal analyzer. Identical powder samples extracted from three parts of a cylindrical specimen cured for 28 days were used for analysis. The powder was obtained by grinding in an agate mortar and then sieved at 75 μm mesh. The samples were then analyzed at a heating rate of 20 °C/min up to 1000 °C, maintaining an isotherm for 10 min for each temperature increase.

2.3.8. Powder X-ray diffraction (XRD)

XRD analysis was performed with a Bruker D2 PHASER instrument with an X-ray tube (Cu 1.54 Å). The diffractogram was obtained over a range of 2θ, varying from 10° to 80°, with a step of 0.061° and at a rate of 1.17° per minute for 60 min. In order to identify the crystalline phases, three identical samples were extracted from a cylindrical test tube after 28 days of curing, which were then ground with an agate mortar until a 75 μm powder was obtained.

2.3.9. Scanning electron microscopy (SEM)

Images of the microstructure of the series were obtained through a HITACHI SU3500 scanning electron microscope (SEM), with a voltage of 10 kV and a working distance of 12 ± 0.2 mm, equipped with a backscattered electron imaging detector and an energy dispersive spectrometer.

3. Results and discussion

3.1. Carbonation

An analysis of the properties obtained in each aggregate, with different initial conditions of accelerated carbonation, is presented below.

3.1.1. Density, absorption, and mass gain

Figs. 4 and 5 present the results for aggregates exposed at carbonation, comparing the density and absorption in two variables studies. Fig. 4 presents all series when exposed to 3 h of the carbonation process and Fig. 5 compares all the series with the same humidity but different exposure times. As the duration of the carbonation process increased, all of the aggregates evaluated increased in density and decreased in absorption but, when the initial humidity of the aggregate changed, the density showed a tendency to increase toward the center and then decrease, and vice versa in the case of the absorption. The P05 aggregates, when exposed to carbon dioxide and an initial humidity between 2.5% and 10% for 3 h, showed a gradual increase in density with increasing initial humidity, densifying the matrix by up to 13% (compared with the sample without initial water). When the initial moisture content of the carbonation process was 10%, the highest density was achieved (1.96 g/cm^3). Compared to the other initial humidities studied in Fig. 4, this effect was less noticeable. In the case of the P07 aggregates, the highest aggregate densification occurred for an initial moisture content of 20% for carbonation, causing an increase of 12.8% of the aggregate. This difference in surface densification caused by carbonation, depending on the original w/c ratio, is explained by the fact that aggregates from a cement paste with a higher w/c ratio have greater microporosity (Lafhaj et al., 2006). This would allow a better diffusivity between CO_2 and the hydration products in the cementitious matrix likely to react with this gas (Song et al., 2006). According to

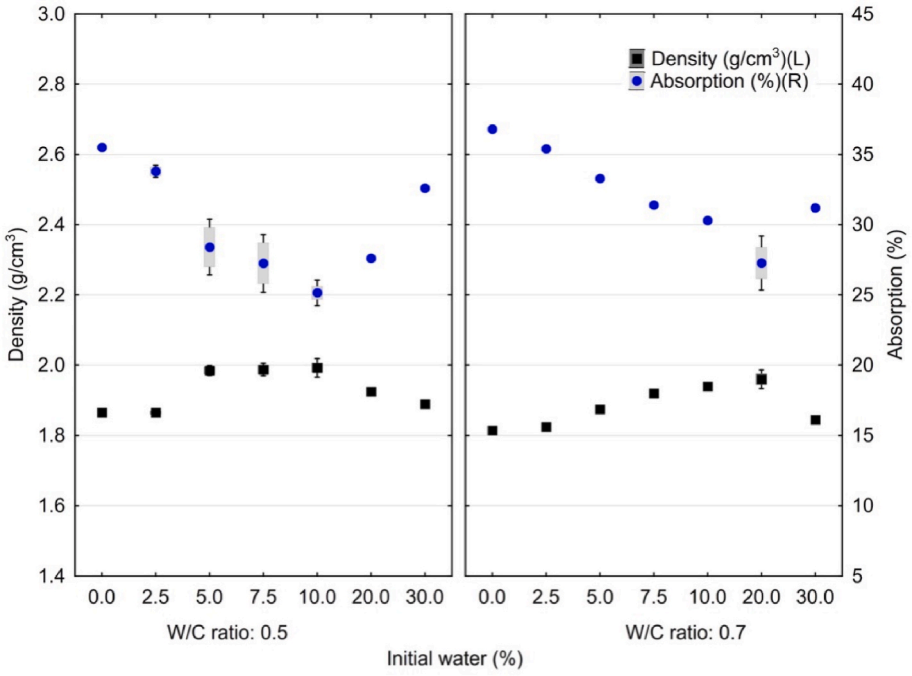

Fig. 4. Effect of initial water in model aggregate and post carbonation absorption results.

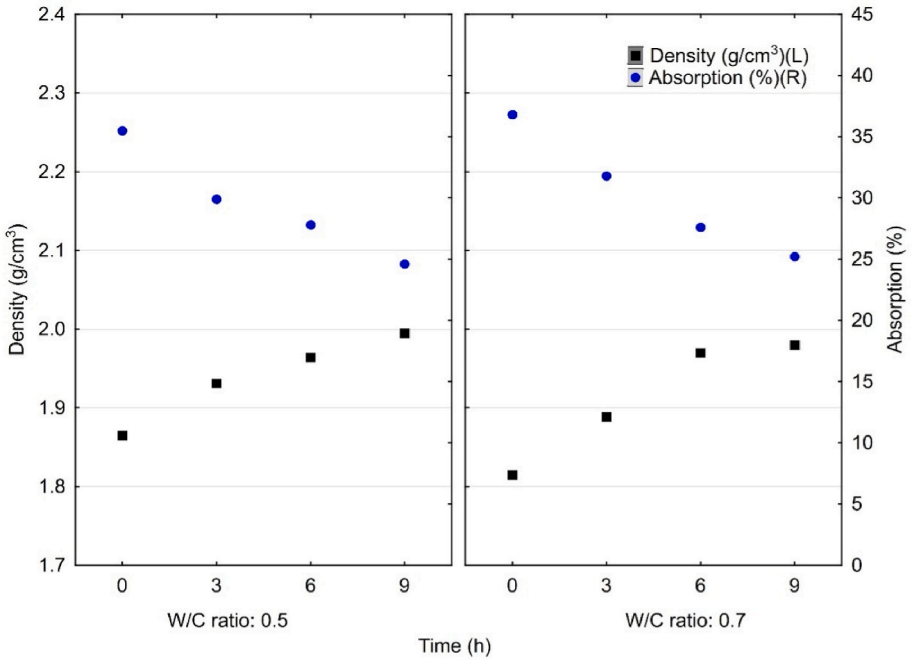

Fig. 5. Effect of carbonation time on aggregate absorption and density results.

Morandeau et al. (2014), the maximum level of carbonation that can be achieved within a cementitious matrix depends not only on the CH and CSH content but also on the accessibility possessed by the hydration products (Morandeau et al., 2014). After studying different w/c ratios (0.45 and 0.60), the accessibility of hydration products was lower in the lower w/c ratio paste because it possessed a denser matrix, the portlandite crystals contained in the paste being more embedded in the matrix. By contrast, the higher w/c ratios indicated that the formation resulted in higher capillary porosity, since the hydration products have better accessibility to these pores, where calcite precipitates.

As for absorption, the increase in the density of the samples due to the reaction of the cement paste aggregates with carbon dioxide was reflected in the decrease of open pores on their surface. This led to a reduction in the absorption of the model aggregates. In the case of the P05 aggregates, the absorption decreased from 35.5% (in the aggregate without any carbonation process) to 24.6% (for the aggregates carbonated for 9 h). For the case of the P07 aggregates, considering the fact that they had an initial absorption of 36.8% before the process, the aggregates exposed to carbonation for 3 h obtained absorption decreases of 14.7%, 17.7%, and 21.2% for initial water percentages of 7.5%, 10%, and 20%, respectively.

According to the results, in both types of aggregates, both the

decrease in density and the increase in absorption were more noticeable when the initial water before carbonation was greater. This is related to the effect that water has on the diffusion and dissolution of CO_2 on the surface of the aggregate. The carbonation process can be divided into three steps: (i) the diffusion of carbon dioxide into the pore of the cementitious matrix, (ii) the dissolution between this gas and CH with CSH and, finally, (iii) the reaction of dissolved carbon dioxide and Ca^{2+} to form calcium carbonate (Zhang et al., 2023). This would only occur effectively when there is an optimal amount of water on the surface of the aggregate. According to Fang and Chang (2015), exceeding this water content leads to blockage of the reaction between CO_2 and the particles in the aggregate due to the excess water in the pores (Chang, 2015); this hinders the first step of carbonation and, thus, the subsequent steps. By contrast, being below the optimal water content implies that the second carbonation step is not completely performed, since only part of the CO_2 can be dissolved with CH and CSH (Chang, 2015). According to the results presented in Fig. 4, this work shows a trend of decreasing absorption as the initial amount of water is higher. However, this property increases when 10% of the initial water is exceeded in the P05 aggregates and 20% in the P07 aggregates. This leads to the conclusion that these values were conducive to improving the characteristics of the aggregates.

On the other hand, as shown in Fig. 5, the processing time also reflected a trend: the longer the carbonation time, the higher the density increase. However, the highest carbonation efficiency is shown within the first 6 h, where the density of the P07 aggregates after 9 h of carbonation is only slightly higher than that after 6 h of carbonation. This was similar to the P05 aggregates, which had a variation of 1.1% between the two durations. Based on this, and considering that industrial processes require limited times, it was decided to set the parameters for both pastes to 6 h.

3.1.2. XRD analysis

After the first phase, X-ray diffraction was performed for both types of recycled cement paste aggregates (P05 and P07) and their carbonate twin samples (P05-C and P07-C). Fig. 6 shows aggregates P05 and P07, which present similar calcite peaks. This was not the case for the portlandite, where the P07 aggregates had higher peaks. According to Slamečka and Škvára (2002), a higher w/c ratio implies a greater free calcium hydroxide content being present on the aggregate surface, which is also related to the permeability of the pastes, thus allowing the passage of water through the anhydrous cement. Compared to the untreated aggregates, both P05-C and P07-C have higher calcite peaks and lower portlandite peaks, reflecting the reaction between hydration products and carbon dioxide (Greve-Dierfeld et al., 2020). This is also related to the increase in the density of the aforementioned mixtures, mainly due to the reaction produced by accelerated carbonation since, as was pointed out by Goyal and Sharma (2018), one of the effects produced by calcite from carbonation in cementitious mixtures is densification (Goyal and Sharma, 2018).

3.2. Effect on mortar specimens

3.2.1. Consistency

Fig. 7 shows the consistency results of the mortars in a fresh state. The control mortar was made with a cement/sand ratio of 1:3 and the necessary water to achieve a consistency of 205 ± 2 mm. In the case of the series with natural sand replacement, as reported in the literature (Martínez et al., 2016),the increase in the replacement percentage by model aggregates meant an increase in the amount of water required to maintain a similar consistency of 205 ± 2 mm. This increase was felt to be more pronounced in the series of mortars with non-carbonated model aggregate replacement. However, compared to the non-carbonated FRA, the accelerated carbonation process reduced the mixing water due to the discussed porosity of the aggregates.

3.2.2. Density, absorption, and porosity

The density, absorption, and porosity results are presented in Figs. 8–10, respectively. As illustrated, the series manufactured with model aggregates obtained lower densities and, therefore, higher porosities and absorptions than the control sample. Considering that the P05 aggregates are denser than the P07 aggregates, the higher the rate of replacement by model aggregates, the more the density of the samples decreased. Therefore, the lower w/c ratio in the original aggregates will result in a lower mix density. In the case of mortars with P05 replacement, the density reduction reached 20% when all the natural aggregates were replaced. Both porosity and absorption were increased by more than 300% and 200%, respectively, for the same series with 100% P05 model aggregates. This effect was increased in the mortars manufactured with 100% P07 model aggregates, with the densities of the S8 samples being lower than the C00 series by 27.38%. However, the effect of accelerated carbonation on the aggregates increased the density of the cementitious matrix of the mortars, affecting the samples with model aggregate replacements with a higher original w/c ratio, more than the twin series with non-carbonated aggregate replacements, with increases of 2.32% for P05-C and 8.84% for P07-C aggregates.

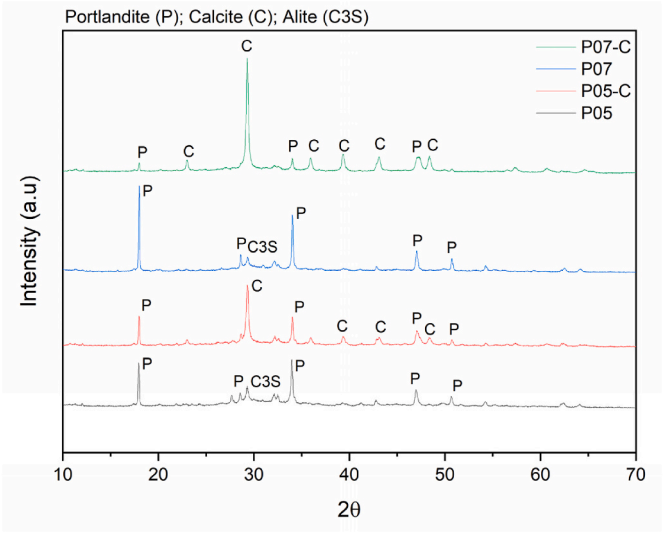

Fig. 6. Results of XRD of model aggregates.

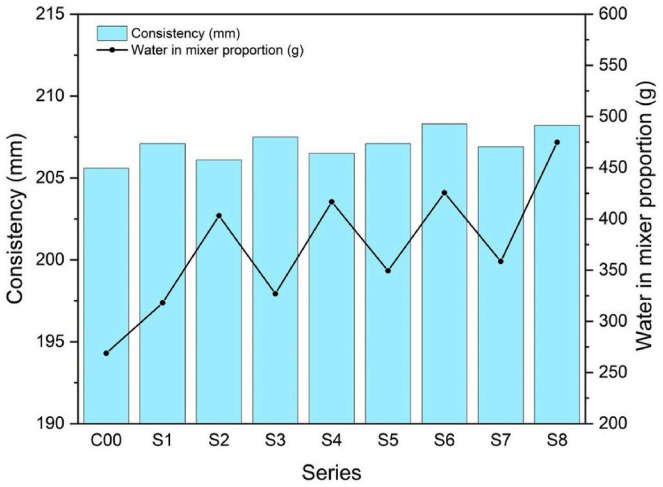

Fig. 7. Consistency results for the manufactured mortars.

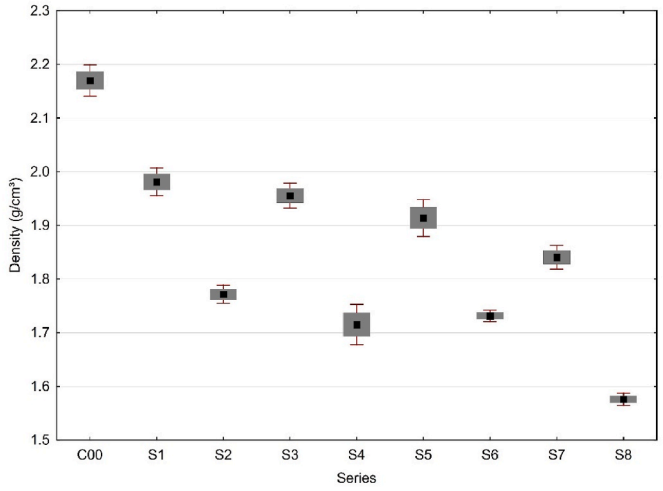

Fig. 8. Density results of mortars.

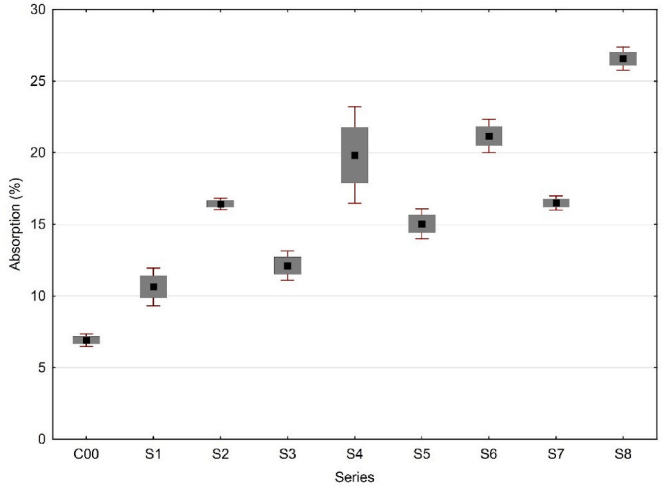

Fig. 9. Absorption results of mortars.

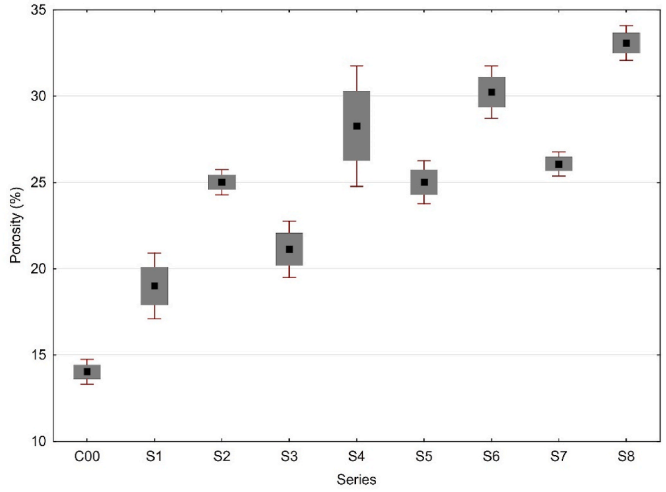

Fig. 10. Porosity results of mortars.

3.2.3. *Compressive and flexural strength*

Fig. 11 shows the compressive strength results of the mortars. As expected from the absorption and density results, as the days of curing progressed, the control series achieved the highest compressive strengths, reaching 45.28 MPa at 28 days. The series with 50% carbonated recycled aggregate replacement obtained decreases of 12.77% and 20.68% for aggregates with P05-C and P07-C, respectively. In contrast, for non-carbonated aggregates, this decrease was 33.82% and 55.79% for replacements by P05 and P07 aggregates, respectively. When the replacement was increased to 100%, the mechanical performance of the mortars decreased even more, being mostly affected in the mortars with P07 aggregate replacements. Thus, the S2 series (with 100% recycled carbonated aggregates from cement pastes with a w/c ratio of 0.5) obtained an average strength of 31.36 MPa. In comparison, the S4 series (with 100% carbonated model aggregates from cement pastes with a W/C ratio of 0.7) achieved an average strength of 29.25 MPa.

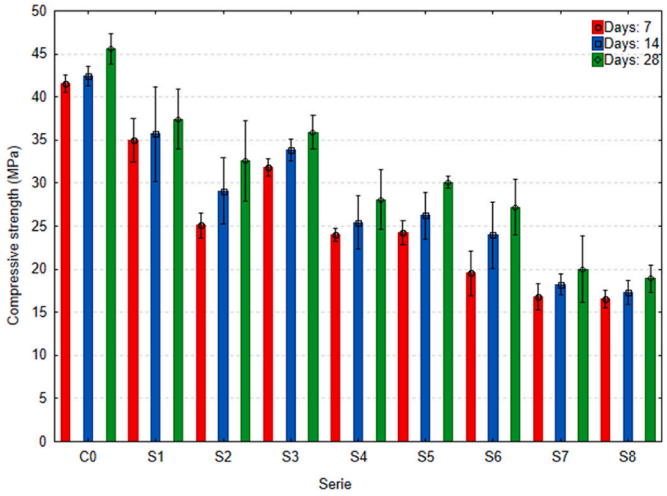

Fig. 11. Results of compressive strength in mortars.

Non-carbonated aggregates showed higher water absorption and lower density than natural aggregate and carbonated aggregates, so they have weaker ITZ when introduced in new mortars. The weakest zone in mortar with model aggregate is ITZ with cement paste (Ma et al., 2023). In this case, based on the results that show an improvement in mechanical performance, it is possible that the carbonation process enhanced the bonding with the cementitious matrix, which could be a new topic to be investigated in future research. Therefore, if we compare the P05 and P05-C series, carbonation increased compressive strengths by 31.81% and 7.76%, for the series with 50% and 100% aggregate replacement, respectively. Conversely, in the series with P07-C aggregates with 50% and 100% replacement, the results were increased by 79.40% and 59.21%, respectively, compared to those presented by the P07 aggregates. Therefore, carbonation is more effective at a higher original w/c ratio, increasing the mechanical properties to a greater extent, which, as previously mentioned, is due to the higher porosity of P07, since it allows greater accessibility of CO_2 and, therefore, a greater formation of carbonation products.

However, leaving aside the carbonation process, the series where the P05 aggregates were incorporated behaved better mechanically than the series with the replacement of the P07 aggregates. This is related to the greater strength of the original pastes and to the formation of more compact ITZ in the new cementitious pastes, similar to that reported by Slamečka and Škvára (2002) who, after examining the effect of the water-cement ratio between 0.19 and 0.50 on the composition and morphology of hydrated cement pastes, indicated that the strength increases with the decrease in w/c.

Fig. 12 shows that the flexural strength results followed the same trend as the compressive strength. The control series had the greatest strength, reaching 7.09 MPa at 28 days. Compared to the control series, Series S1 and S2 (with P05-C aggregates) showed decreases of 7.4% and

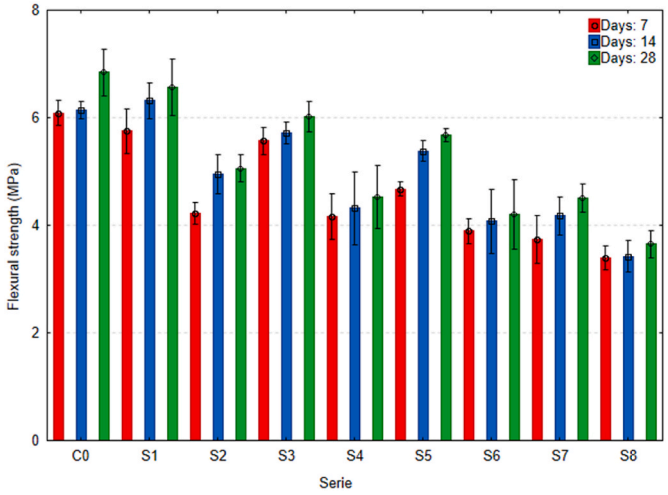

Fig. 12. Results of flexural strength in mortars.

27.15% for 50% and 100% replacements, respectively. Meanwhile, the series with P07-C aggregates had a strength of 5.93 MPa (S3) and 4.26 MPa (S4) for 50% and 100% replacements, respectively, being lower than the C00 series by 16.43% and 39.92%.

In the case of compressive strength, as a result of the accelerated carbonation in the aggregates, there was an increase in flexural strength compared to their non-carbonated series, improving this property by 15.07% and 22.68% for the S1 and S2 series, respectively. In the case of P07 aggregates, this characteristic increased by 29.65% and 21.54%, compared to the S7 and S8 series with non-carbonated aggregates.

As noted, the flexural strength was less affected than the compressive strength. However, both properties had a similar behavioral trend, outperforming their untreated counterparts. This was mainly due to the increase in density and the decrease in micropores because of carbonation, which gave the aggregates a better mechanical capacity.

3.2.4. Ultrasonic pulse velocity

The ultrasonic pulse velocities obtained in the mortars are presented in Fig. 13. As with the other properties, the results show that accelerated carbonation caused an improvement in this property. The series manufactured with carbonated aggregates showed an increase of about 11% over the non-carbonated series.

The series where the total natural aggregates were replaced by P05 and P07 aggregates obtained the lowest UPVs (below 3000 m/s). In

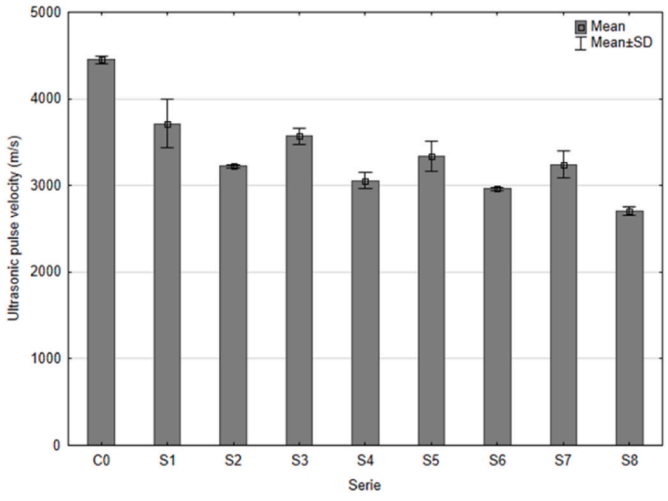

Fig. 13. Ultrasonic pulse velocity of mortars.

comparison, the series with 100% replacement by carbonate aggregates (P05-C and P07-C) exceeded that range with velocities between 3222 m/s and 3057 m/s, respectively. When 50% of the natural aggregates were replaced, the maximum UPV velocities were achieved. Although none of the series manufactured with model aggregates outperformed the control series, the highest speeds were obtained by the S1 and S3 series, which reached 3876 m/s and 3571 m/s, respectively. This is directly related to the development of matrix densification presented above, since a higher ultrasonic pulse velocity indicates a decrease in the pores of the cementitious matrix (Zhang et al., 2015). It is then held that calcite precipitation implied a reduction of pores on its surface, such that the ultrasonic wave traveled at a higher velocity through the mortar matrix (Ahn et al., 2017). The pulse velocity has a trend similar to the compressive strength obtained from the mortars (Parsompech et al., 2022).

3.2.5. Microscopic analysis

The SEM analysis performed on the mortars with maximum percentages of carbonated aggregate incorporation is presented at three different magnifications (100, 50, and 20 μm) in Fig. 14. As can be seen, a much 'denser' or visually smoother surface was achieved in the control mortar, while the mortars with carbonated model aggregates had rougher surfaces. Mortars with P07-C aggregates have a (visually) more disordered surface than the others. On the other hand, as the image magnification increases, there is a greater presence of calcite as structured crystals in the S2 series (with P05-C aggregates) but in a less structured way than in the S4 series (with P07-C aggregates). Despite observing the development of calcite, these do not have a crystalline form, in the main, but they have a nucleation matrix with small, flat, and rounded structures associated with thermodynamic stability of the calcite. Wang et al. (2019) indicated that three periods of this mineral can occur. First, the calcite forms a nucleation matrix, then the reaction continues transforming these crystals, increasing their size and forming poorly crystallized calcite. In the third period, crystal sizes increase and thermodynamic stability is achieved (Wang et al., 2019). From the above, it follows that the carbonation obtained did not go beyond the first stage.

On the other hand, in the case of the control mortar, part of the image shows needle-shaped hydration products, which may be associated with the development of ettringite (He et al., 2016). This may imply a greater partial filling of the pores and agrees with the previous results obtained regarding the density and porosity of the samples (He et al., 2016), (Li et al., 2017). However, considering that this test was performed at 28 days of curing, late ettringite formation could result in durability problems. The authors indicate that the presence of these needles can be attributed to the presence of sulfates and alkalis (Coakley, 2014).

3.2.6. TGA analysis

The thermogravimetric analysis of the mortars with P05 aggregate replacements is presented in Fig. 15, while Fig. 16 presents the series with P07 aggregate replacements. In both cases, the first peaks of the DTA curves occur between 150 °C and 200 °C, corresponding to free water evaporation or dehydration of the silica gel and hydration products (CSH) and AFm (Vogler et al., 2022). In this first curve, the series with P05-C aggregate replacements have lower dehydration percentages than mortars with P07-C aggregates because they had lower w/c ratios in their manufacture. Then, between 400 °C and 500 °C, the curve associated with portlandite dehydration occurs (Steiner et al., 2020). As can be seen in both graphs, the series with non-carbonated aggregates (S6, S7, S8, and S9) show higher curves than the series manufactured with carbonated model aggregates. This is because CSH and portlandite are the hydration products with the greatest reactivity to CO_2 (Sharma, 2020). Therefore, after reacting with CO_2, portlandite, in this case, decreases in the series with P05-C and P07-C aggregates.

Finally, between 550 °C and 800 °C, the peak corresponding to calcite decomposition occurs (Xue et al., 2022). As can be seen, and

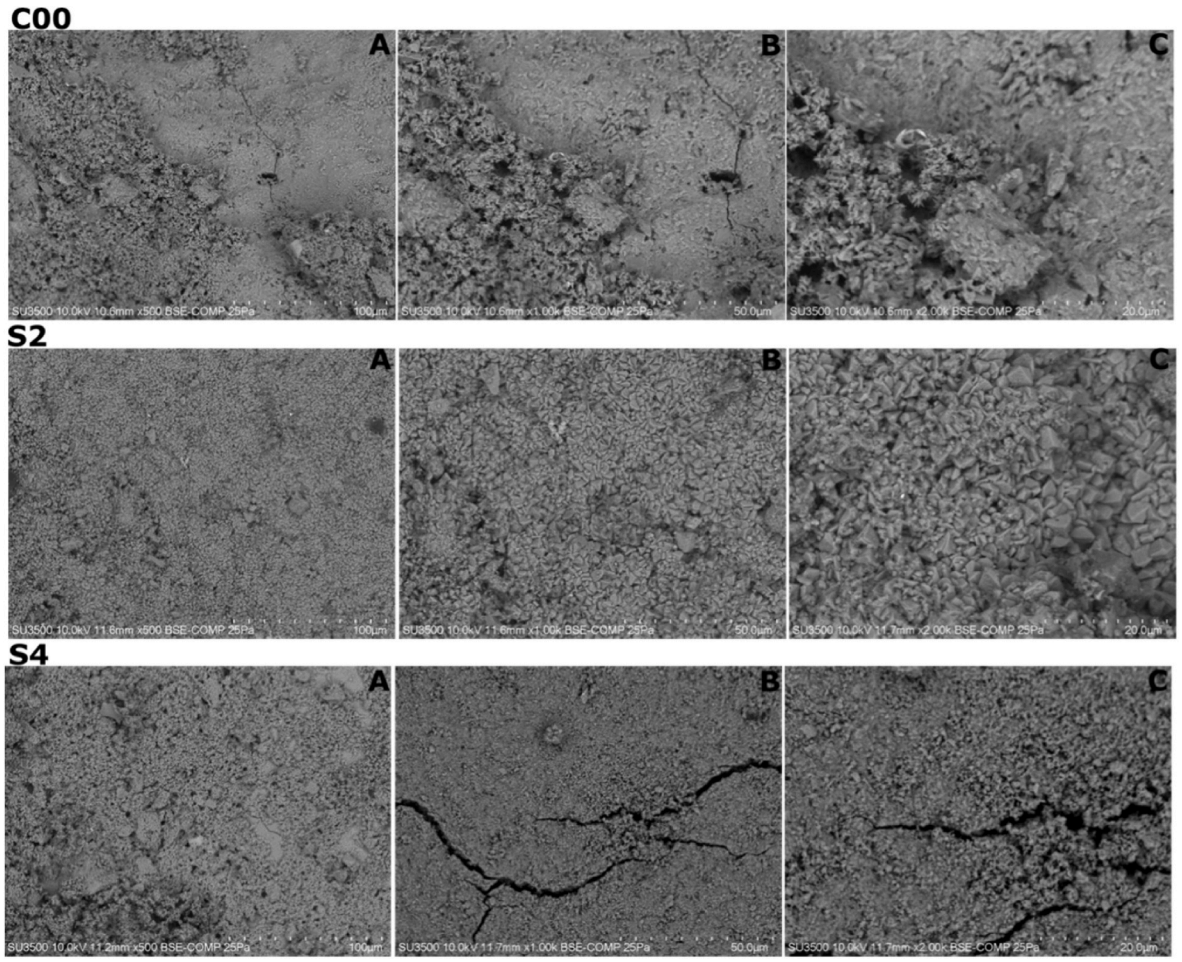

Fig. 14. SEM images of mortars at 100 μm (A) 50 μm (B) and 20 μm (C) magnification.

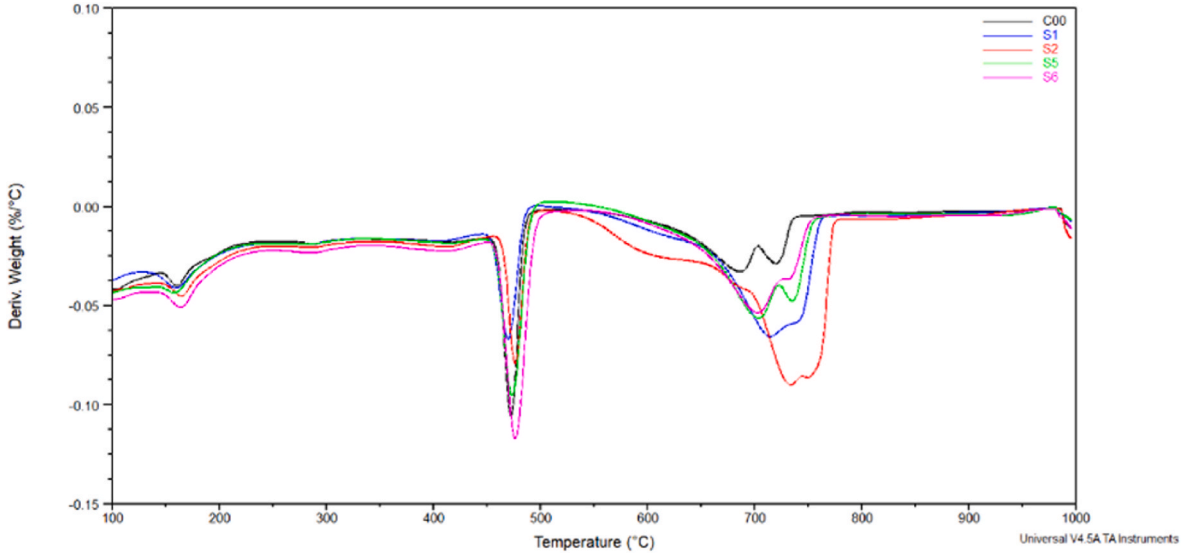

Fig. 15. TGA results of mortars with aggregate replacements P05.

corresponding with the X-ray diffraction results, the series that had a greater decomposition contained replacements by aggregates with carbonated cement paste (Xue et al., 2022). According to Vogler et al. (2022), different carbonate modifications (amorphous carbonates, aragonite and vaterite) can occur in the temperature range from 500 °C to 700 °C. Since they have similar decomposition temperatures, it is difficult to decide which curve they approach (Vogler et al., 2022). However, it is possible to observe differences between both types of mortars, in the results of the mortars made with P07 (Fig. 16) it is possible to observe curves above 700° and smoother, in contrast to the

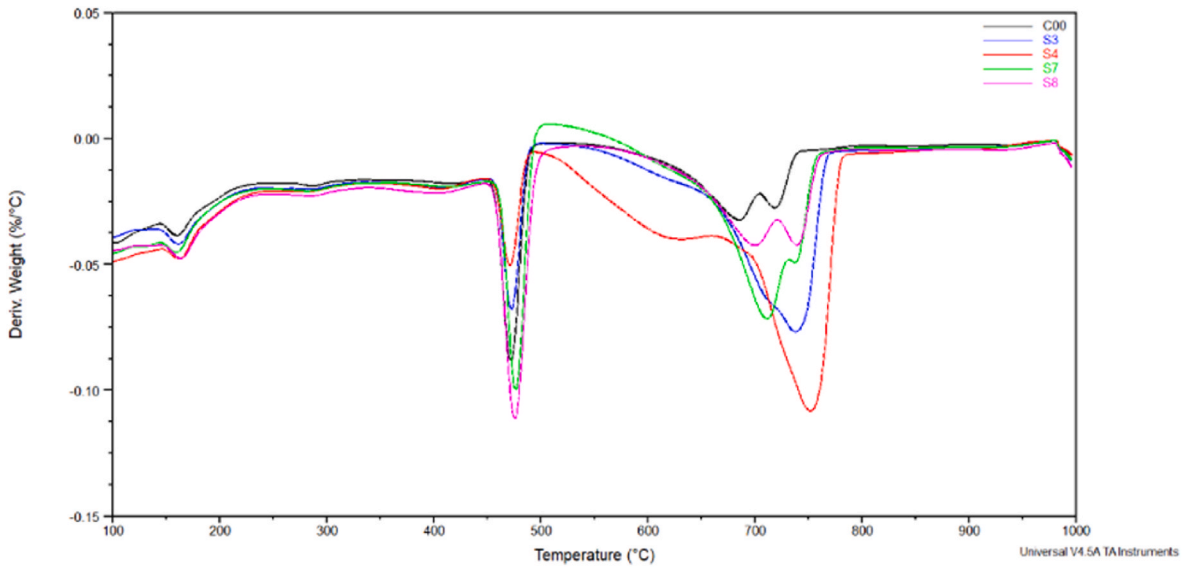

Fig. 16. TGA results of mortars with aggregate replacements P07.

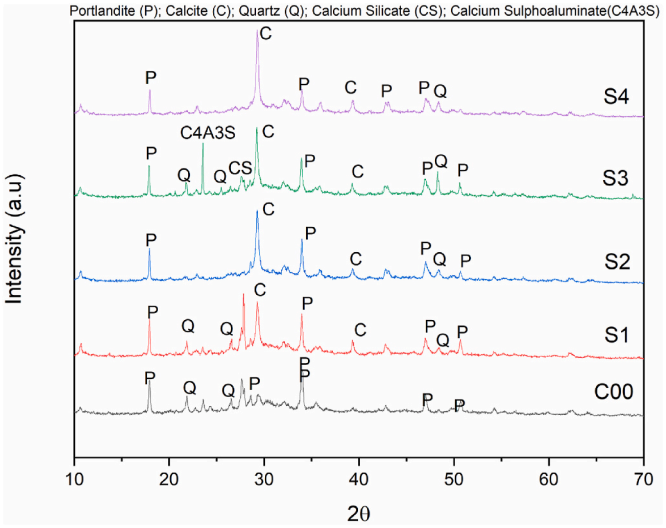

Fig. 17. X-ray diffraction results of mortars with aggregate replacements P07.

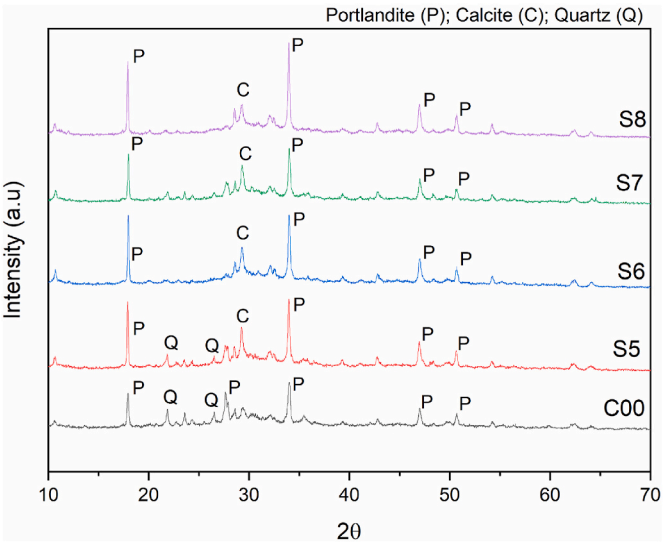

Fig. 18. X-ray diffraction results of mortars with aggregate replacements P05.

mortars made with P05 (Fig. 17), with wider curves and in lower decomposition temperatures. Taking this into account, it can be seen that the S3 and S4 series have a higher carbonate crystallinity compared to the control series.

3.2.7. XRD analysis

Fig. 17 presents X-ray diffraction results separately for the series with carbonated aggregates, while Fig. 18 presents the series with non-carbonated aggregates. The presence of portlandite and quartz is distinguished in all the series with similar peak intensities due to the cementitious mixture prepared with aggregates of siliceous origin. However, the difference is in the calcite. This compound is precipitated by accelerated carbonation in the model aggregates but is absent in the control series. Therefore, it is also possible to distinguish that in the series with a higher replacement percentage, the presence of the calcite peak is higher, which is in line with the TGA results. Regarding the type of model aggregate, it is possible to distinguish that, compared to the S2 series manufactured with P05-C aggregates, the S4 series (manufactured with P07-C aggregates) has a higher calcite intensity, which is related to what was previously mentioned; the physical results associated with the porosity of these aggregates imply higher calcite precipitation. Therefore, there is a greater presence of calcite in the mortars.

3.2.8. Carbon dioxide sequestration capacity

Fig. 19 shows the results associated with the sequestering capacity of the different series of mortars. As aggregate replacement increased, so did sequestration capacity, most notably in the series using carbonated aggregates. The highest calculated rate was for the series with 100% replacement of P07-C aggregates, exceeding the control series by 226% of CO_2 sequestration. The P05-C aggregate achieved a rate of 16.4 g/kg of aggregate when its replacement rate was 100%. This is related to the previous discussion: a higher w/c ratio in the aggregate meant a higher carbonation. Compared to the control series, the carbonation process in the aggregates increased this capacity by 31% (S2) and 58% (S4), for the series where 100% of the aggregates were replaced.

4. Conclusions

The current study evaluated the behavior of two model aggregates

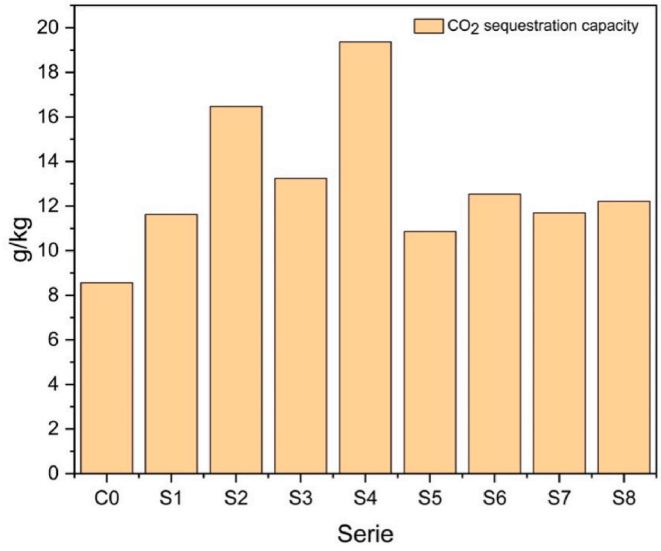

Fig. 19. Sequestration capacity results of mortars.

from cementitious pastes with varying water-cement ratios subjected to an accelerated carbonation process, in order to analyze the variables that control carbonation. It also assessed how well these carbonated cement paste model aggregates performed in mortars that replaced natural aggregates by 50% and 100% of their volume. Based on the results obtained in this research, it can be concluded that:

- The accelerated carbonation process positively influences the density and absorption properties of model aggregates. However, due to the heterogeneity that can occur in these materials, it is necessary to evaluate the conditions under which the process will be performed beforehand. On this occasion, the higher origin w/c ratio required higher amounts of initial moisture content in the carbonation process. Similarly, the improvement process in recycled aggregates from the carbonation process may be more evident in recycled aggregates from more porous, low-strength concrete or cementitious pastes. The higher surface porosity allows carbon dioxide to enter the matrix and seal more pores.
- Concerning the mortars manufactured with model aggregates, none of the series were able to match the physical properties of the control series. Lower densities and, therefore, higher porosities and absorptions were obtained. However, the effect of accelerated carbonation on the aggregates managed to increase the density of the cementitious matrix of the mortars, having a greater effect on the samples with replacements of model aggregates with higher original w/c ratios. They increased by 2.32% for the case of P05-C and 8.84% of P07-C aggregates compared to the twin series of non-carbonated aggregates. A similar effect occurred with the consistency of the mixes, where the accelerated carbonation process decreased the w/c ratio by 5% and 13% for the P05-C and P07-C aggregates, respectively.
- Regarding the mechanical performance of the mortars, the series where 50% of carbonate aggregates were replaced obtained decreases of 12.77% and 20.68% in compressive strength for aggregates with P05-C and P07-C, respectively. These are positive results, considering the reductions in the twin samples manufactured with aggregates without carbonation treatment. Regarding the original w/c ratio, the series incorporating P05 aggregates achieved better mechanical behavior than the series with the P07 aggregate replacement, which is related to the formation of more compact ITZ in the new cementitious pastes. Flexural strength results followed a similar trend. The control series obtained the greatest strength, reaching 7.09 MPa at 28 days. Performance decreased by 7.4% and 16.43% for 50% replacements of P05-C and P07-C aggregates, respectively.
- Similar to what was indicated for the other properties, the results show that accelerated carbonation caused an improvement in the UPV in the mortars, increasing speeds by 11% in the series with carbonated aggregates, compared to the series with non-carbonated aggregates. On the other hand, the thermal conductivity results obtained were not affected by the carbonation process applied to the aggregates.
- TGA and XRD analysis confirmed that the accelerated carbonation process resulted in calcite precipitation in the aggregates. At the same time, the CO_2 sequestration capacity (g/kg) was calculated in the mortars and expressed as grams of CO_2 sequestered per 1 kg of sample. The process performed on the cement paste model aggregates increased this capacity in the mortars, being higher for aggregates with a higher original w/c ratio. The S2 and S4 series yielded 31% and 58% increases compared to the twin series with non-carbonated aggregate replacements.

CRediT authorship contribution statement

Marion Bustamante: Writing – original draft, Methodology, Investigation, Funding acquisition, Data curation. **Viviana Letelier:** Writing – review & editing, Supervision, Methodology, Investigation, Data curation, Conceptualization. **Bruno Wenzel:** Writing – review & editing, Methodology, Conceptualization. **Cristian Torres:** Investigation, Data curation. **Estefania Loyola:** Methodology, Investigation. **José Marcos Ortega:** Methodology, Conceptualization.

Declaration of competing interest

The authors declare that they have no known competing financial interests or personal relationships that could have appeared to influence the work reported in this paper.

Data availability

No data was used for the research described in the article.

Acknowledgments

This work was supported by the Agencia Nacional de Investigación y Desarrollo de Chile (ANID) under Grant No. FONDECYT REGULAR 1211135 and Grant No. Beca Doctorado Nacional 21231311. Additionally, the authors gratefully acknowledge the partial support from Universidad de La Frontera (Chile) and Ministerio de Educación (MINEDUC) (Project FRO2395).

References

A. (American S. for Testing y Materials), 2021. «C78/C78M standard test method for flexural strength of concrete (Using simple beam with third-point loading) [En línea]. Disponible en: https://www.astm.org/c0078_c0078m-18.html.

A. (American S. for Testing y Materials), 2023. C39/C39M - 21 - Standard Test Method for Compressive Strength of Cylindrical Concrete Specimens1 [En línea]. Disponible en:. https://compass.astm.org/document/?contentCode=ASTM%7CC0039_C0039M-21%7Cen-US&proxycl=https%3A%2F%2Fsecure.astm.org&fromLogin=true.

A. (American S. for Testing y Materials), «C595 Standard Specification for Blended Hydraulic Cements». [En línea]. Disponible en: https://www.astm.org/standards/c595.

A. (American S. for Testing y Materials). ASTM E104-20a [En línea]. Disponible en. https://www.techstreet.com/standards/astm-e104-20a?product_id=2203246.

A. (American S. for Testing y Materials). C597-16 - Standard Test Method for Pulse Velocity Through Concrete [En línea]. Disponible en. https://www.astm.org/c0597-16.html.

A. E. de N. y Certificación, 2000a. UNE-EN 1015-10 métodos de ensayo de los morteros para albañilería. Parte 10, Determinación de la densidad aparente en seco del mortero endurecido. AENOR.

A. E. de N. y Certificación, 2000b. UNE-EN 1015-3 métodos de ensayo de los morteros para albañilería. Parte 3, Determinación de la consistencia del mortero fresco (por la mesa de sacudidas). AENOR.
A. E. de N. y Certificación, 2003. UNE-EN 1015-18: métodos de ensayo de los morteros para albañilería. Determinación del coeficiente de absorción de agua por capilaridad del mortero endurecido. AENOR.
Ahn, E., Kim, H., Sim, S.H., Shin, S.W., Shin, y M., 2017. Principles and applications of ultrasonic-based nondestructive methods for self-healing in cementitious materials. Materials 10, 278. https://doi.org/10.3390/MA10030278 vol. 10, n.o 3, p. 278, mar. 2017.
Akhtar, A., Sarmah, y A.K., 2018. Construction and Demolition Waste Generation and Properties of Recycled Aggregate Concrete: A Global Perspective. https://doi.org/10.1016/j.jclepro.2018.03.085.
Chang, Y. Fang y J., 2015. Microstructure changes of waste hydrated cement paste induced by accelerated carbonation. Construct. Build. Mater. 76, 360–365. https://doi.org/10.1016/J.CONBUILDMAT.2014.12.017.
Chang, J., Fang, Y., Shang, y X., 2016. The role of β-C2S and γ-C2S in carbon capture and strength development. Mater. Struct. Constr. 49 (10), 4417–4424. https://doi.org/10.1617/S11527-016-0797-5/TABLES/1.
Coakley, D. Bondar y E., 2014. Use of gypsum and CKD to enhance early age strength of High Volume Fly Ash (HVFA) pastes. Construct. Build. Mater. 71, 93–108. https://doi.org/10.1016/J.CONBUILDMAT.2014.08.015.
Fang, X., Zhan, B., Poon, y C.S., 2020a. Enhancing the accelerated carbonation of recycled concrete aggregates by using reclaimed wastewater from concrete batching plants. Construct. Build. Mater. 239, 117810. https://doi.org/10.1016/j.conbuildmat.2019.117810 abr.
Fang, Y., Liu, Z., Wang, Q., Zhang, Y., Zhang, M., Wang, y Q., 2020b. Strength development and products evolution of β-C2S and γ-C3S induced by accelerated carbonation curing. J. Wuhan Univ. Technol.-Materials Sci. Ed. 35 (6), 1053–1060. https://doi.org/10.1007/s11595-020-2355-9 dic.
Fang, X., Xuan, D., Shen, P., Poon, y C.S., 2021. Fast enhancement of recycled fine aggregates properties by wet carbonation. J. Clean. Prod. 313, 127867. https://doi.org/10.1016/J.JCLEPRO.2021.127867.
Georget, F., Soja, W., Scrivener, y K.L., 2020. Characteristic lengths of the carbonation front in naturally carbonated cement pastes: implications for reactive transport models. Cement Concr. Res. 134, 106080. https://doi.org/10.1016/j.cemconres.2020.106080 ago.
Goyal, D., Sharma, y S., 2018. Accelerated carbonation curing of cement mortars containing cement kiln dust: an effective way of CO2 sequestration and carbon footprint reduction. J. Clean. Prod. 192, 844–854. https://doi.org/10.1016/J.JCLEPRO.2018.05.027.
Greve-Dierfeld, von, et al., 2020. Understanding the carbonation of concrete with supplementary cementitious materials: a critical review by RILEM TC 281-CCC. Mater. Struct. 2021 53 (6), 1–34. https://doi.org/10.1617/S11527-020-01558-W, 536.
Hawileh, R.A., et al., 2023. Properties of concrete replaced with different percentages of recycled aggregates. Mater. Today Proc., abr. https://doi.org/10.1016/j.matpr.2023.03.336.
He, P., Shi, C., Tu, Z., Poon, C.S., Zhang, y J., 2016. Effect of further water curing on compressive strength and microstructure of CO2-cured concrete. Cem. Concr. Compos. 72, 80–88. https://doi.org/10.1016/J.CEMCONCOMP.2016.05.026.
(Instituto Nacional de Normalización) INN, 2001. NCh 2256/1.of 2001, Mortar - Part 1: General Requirements.
International, A., 2013. ASTM C1585-13, Standard Test Method for Measurement of Rate of Absorption of Water by Hydraulic-Cement Concretes. https://doi.org/10.1520/C1585-13.
Kurda, J. de Brito y R., 2021. The past and future of sustainable concrete: a critical review and new strategies on cement-based materials. J. Clean. Prod. 281, 123558. https://doi.org/10.1016/J.JCLEPRO.2020.123558 ene.
Lafhaj, Z., Goueygou, M., Djerbi, A., Kaczmarek, y M., 2006. Correlation between porosity, permeability and ultrasonic parameters of mortar with variable water/cement ratio and water content. Cement Concr. Res. 36 (4), 625–633. https://doi.org/10.1016/J.CEMCONRES.2005.11.009 abr.
Li, L., Poon, C.S., Xiao, J., Xuan, y D., 2017. Effect of carbonated recycled coarse aggregate on the dynamic compressive behavior of recycled aggregate concrete. Construct. Build. Mater. 151, 52–62. https://doi.org/10.1016/j.conbuildmat.2017.06.043.
Li, L., Liu, Q., Huang, T., Peng, y W., 2022. Mineralization and utilization of CO2 in construction and demolition wastes recycling for building materials: a systematic review of recycled concrete aggregate and recycled hardened cement powder. Sep. Purif. Technol. 298, 121512. https://doi.org/10.1016/J.SEPPUR.2022.121512.
Luković, B. Šavija y M., 2016. Carbonation of cement paste: understanding, challenges, and opportunities. Construct. Build. Mater. 117, 285–301. https://doi.org/10.1016/j.conbuildmat.2016.04.138.
Ma, H., Tu, Y., Yu, H., Diao, Y., Han, W., Zhang, y M., 2023. Mechanical properties and microstructural characteristics of coral-aggregate-concrete ITZ: experimental study. J. Build. Eng. 72, 106647. https://doi.org/10.1016/j.jobe.2023.106647 ago.
Martínez, P.S., Cortina, M.G., Martínez, F.F., Sánchez, y A.R., 2016. Comparative study of three types of fine recycled aggregates from construction and demolition waste (CDW), and their use in masonry mortar fabrication. J. Clean. Prod. 118, 162–169. https://doi.org/10.1016/J.JCLEPRO.2016.01.059.
Liu, Z., Meng, W., 2021. Fundamental understanding of carbonation curing and durability of carbonation-cured cement-based composites: a review. J. CO2 Util. 44, 101428. https://doi.org/10.1016/J.JCOU.2020.101428.
Mi, R., Yu, T., Poon, y C.S., 2023a. Feasibility of utilising porous aggregates for carbon sequestration in concrete. Environ. Res. 228, 115924. https://doi.org/10.1016/j.envres.2023.115924.
Mi, R., Wang, Y., Yu, T., Li, y W., 2023b. Effects of carbon-sequestering coral aggregate on pore structures and compressive strength of concrete. Low-Carbon Mater. Green Constr. 1 (1), 21. https://doi.org/10.1007/s44242-023-00024-4.
Morandeau, A., Thiéry, M., Dangla, y P., 2014. Investigation of the carbonation mechanism of CH and C-S-H in terms of kinetics, microstructure changes and moisture properties. Cement Concr. Res. 56, 153–170. https://doi.org/10.1016/J.CEMCONRES.2013.11.015.
Parsompech, N., Rianyoi, R., Chaipanich, y A., 2022. Compressive strength, water absorption and pulse velocity tests of calcined clay- limestone cement mortars. Mater. Today Proc. 65, 2394–2398. https://doi.org/10.1016/J.MATPR.2022.05.526.
Poon, C.S., Shen, P., Jiang, Y., Ma, Z., Xuan, y D., 2023. Total recycling of concrete waste using accelerated carbonation: a review. Cement Concr. Res. 173, 107284. https://doi.org/10.1016/J.CEMCONRES.2023.107284.
Rostami, V., Shao, Y., Boyd, A.J., He, y Z., 2012. Microstructure of cement paste subject to early carbonation curing. Cement Concr. Res. 42 (1), 186–193. https://doi.org/10.1016/j.cemconres.2011.09.010.
Sharma, S. Goyal y D., 2020. CO2 sequestration on cement. In: Start- Creat. Smart Eco-Effic. Built Environ, second ed., pp. 109–142. https://doi.org/10.1016/B978-0-12-819946-6.00006-0 ene.
Shen, P., et al., 2022. Phase assemblance evolution during wet carbonation of recycled concrete fines. Cement Concr. Res. 154, 106733. https://doi.org/10.1016/j.cemconres.2022.106733 abr.
Shtepenko, O., Hills, C., Brough, A., Thomas, y M., 2006. The effect of carbon dioxide on β-dicalcium silicate and Portland cement. Chem. Eng. J. 118 (1–2), 107–118. https://doi.org/10.1016/J.CEJ.2006.02.005.
Slamečka, T., Škvára, F., 2002. The effect of water ratio on microstructre and composition of the hydration products of portland cement pastes. Ceram. – Silikáty 46 (4), 152–158.
Song, H.W., Kwon, S.J., Byun, K.J., Park, y C.K., 2006. Predicting carbonation in early-aged cracked concrete. Cement Concr. Res. 36 (5), 979–989. https://doi.org/10.1016/J.CEMCONRES.2005.12.019.
Sousa, L.N., Zepper, J.C.O., Schollbach, K., Brouwers, y H.J. H., 2024. Improving the reactivity of industrial recycled concrete fines: exploring mechanical and hydrothermal activation. Construct. Build. Mater. 442, 137594. https://doi.org/10.1016/j.conbuildmat.2024.137594.
Steiner, S., Lothenbach, B., Proske, T., Borgschulte, A., Winnefeld, y F., 2020. Effect of relative humidity on the carbonation rate of portlandite, calcium silicate hydrates and ettringite. Cement Concr. Res. 135, 106116. https://doi.org/10.1016/J.CEMCONRES.2020.106116.
Illankoon, I.M.C.S., Tam, V.Y., 2021. Life Cycle Costing for Decision Making in Construction and Demolition Waste Management: A Critical Review, pp. 163–169. https://doi.org/10.1007/978-3-030-48465-1_28.
Tam, V.W.Y., Wattage, H., Le, K.N., Buteraa, A., Soomro, y M., 2021. «Methods to Improve Microstructural Properties of Recycled Concrete Aggregate: A Critical Review», Construction and Building Materials, vol. 270. Elsevier Ltd, 121490. https://doi.org/10.1016/j.conbuildmat.2020.121490 febrero de.
Vogler, N., Drabetzki, P., Lindemann, M., Kühne, y H.C., 2022. Description of the concrete carbonation process with adjusted depth-resolved thermogravimetric analysis. J. Therm. Anal. Calorim. 147 (11), 6167–6180. https://doi.org/10.1007/S10973-021-10966-1/TABLES/2.
Wang, D., Fang, Y., Zhang, Y., Chang, y J., 2019. Changes in mineral composition, growth of calcite crystal, and promotion of physico-chemical properties induced by carbonation of β-C2S. J. CO2 Util. 34, 149–162. https://doi.org/10.1016/J.JCOU.2019.06.005.
Xiao, J., 2018. Recycled Aggregate Concrete Structures. Springer T. https://doi.org/10.1007/978-3-662-53987-3_16.
Xiao, J., Li, W., Corr, D.J., Shah, y S.P., 2013. Effects of interfacial transition zones on the stress–strain behavior of modeled recycled aggregate concrete. Cement Concr. Res. 52, 82–99. https://doi.org/10.1016/j.cemconres.2013.05.004.
Xiao, J., Zhang, H., Tang, Y., Deng, Q., Wang, D., sun Poon, y C., 2022. Fully utilizing carbonated recycled aggregates in concrete: strength, drying shrinkage and carbon emissions analysis. J. Clean. Prod. 377, 134520. https://doi.org/10.1016/J.JCLEPRO.2022.134520 dic.
Xuan, D., Poon, y C.S., 2019. «16 - Sequestration of carbon dioxide by RCAs and enhancement of properties of RAC by accelerated carbonation», en New Trends in Eco-efficient and Recycled Concrete. In: Agrela, J. de Brito y F. (Ed.), en Woodhead Publishing Series in Civil and Structural Engineering. Woodhead Publishing, pp. 477–497. https://doi.org/10.1016/B978-0-08-102480-5.00016-6.
Xue, K., Wan, C., Xu, Y., Jiang, Y., Cheng, y Y., 2022. Effect of pre-hydration age on phase assemblage, microstructure and compressive strength of CO2 cured cement mortar. Construct. Build. Mater. 325, 126760. https://doi.org/10.1016/J.CONBUILDMAT.2022.126760.
Zadeh, A.H., Mamirov, M., Kim, S., Hu, y J., 2021. CO2-treatment of recycled concrete aggregates to improve mechanical and environmental properties for unbound applications. Construct. Build. Mater. 275, 122180. https://doi.org/10.1016/J.CONBUILDMAT.2020.122180.
Zhang, J., Shi, C., Li, Y., Pan, X., Poon, C.S., Xie, y Z., 2015. Influence of carbonated recycled concrete aggregate on properties of cement mortar. Construct. Build. Mater. 98, 1–7. https://doi.org/10.1016/J.CONBUILDMAT.2015.08.087.

Zhang, D., Ghouleh, Z., Shao, y Y., 2017. Review on carbonation curing of cement-based materials. J. CO2 Util. 21, 119–131. https://doi.org/10.1016/J.JCOU.2017.07.003.
Zhang, L.W., Sojobi, A.O., Kodur, V.K.R., Liew, y K.M., 2019. Effective utilization and recycling of mixed recycled aggregates for a greener environment. J. Clean. Prod. 236, 117600. https://doi.org/10.1016/J.JCLEPRO.2019.07.075.
Zhang, T., Chen, M., Wang, Y., Zhang, y M., 2023. Roles of carbonated recycled fines and aggregates in hydration, microstructure and mechanical properties of concrete: a critical review. Cem. Concr. Compos. 138, 104994. https://doi.org/10.1016/j.cemconcomp.2023.104994 abr.